EARTHQUAKE ENGINEERING AND STRUCTURAL DYNAMICS, VOL. 26, 1137–1156 (1997)

SLIDING MODE CONTROL WITH COMPENSATOR FOR WIND AND SEISMIC RESPONSE CONTROL

J. N. YANG,[1]* J. C. WU,[2] A. K. AGRAWAL[3] AND S. Y. HSU[3]

[1]*Department of Civil and Environmental Engineering, University of California, Irvine, CA 92697, U.S.A.*
[2]*Department of Civil Engineering, Tamkang University, Taipei, Taiwan*
[3]*Department of Civil and Environmental Engineering, University of California, Irvine, CA 92697, U.S.A.*

SUMMARY

Recently, it has been demonstrated that control techniques based on sliding mode control (SMC) are robust and their performances are quite remarkable for applications to active/hybrid control of seismic-excited linear, non-linear or hysteretic civil engineering structures. In this paper, sliding mode control methods are further extended by introducing a compensator. The incorporation of a compensator provides (i) a convenient way of making trade-offs between control efforts and specific response quantities of the structure through the use of linear quadratic optimal control theory, and (ii) a convenient design procedure for static output feedback controllers to facilitate practical implementations of control systems. Since civil engineering structures generally involve excessive degrees of freedom, a controller design based on a full-order system may be difficult, in particular for wind-excited tall buildings. In this paper, three reduced-order control methods have been used and their performances have been investigated. Applications of sliding mode control with compensators to active control of buildings subject to either earthquakes or strong wind gusts have been demonstrated through numerical simulations. Simulation results show that the performance of the sliding mode controller with compensators for the reduced-order system is quite close to that of the controller based on the full-order system as long as enough vibrational modes are taken into account in the reduced-order system. © 1997 John Wiley & Sons, Ltd.

Earthquake Engng. Struct. Dyn., **26**, 1137–1156 (1997)

No. of Figures: 2. No. of Tables: 6. No. of References: 37.

KEY WORDS: sliding mode control; compensator; reduced-order system; seismic response control; wind response control; critical-mode control

1. INTRODUCTION

Active/hybrid control of tall buildings and long-span bridges subject to seismic excitations or strong wind turbulences has received considerable attention among researchers. In particular, different control methods have been investigated and control devices have been installed on some new buildings in Japan (e.g. Reference 1). Recently, various advanced control theories have been investigated for implementations of active/hybrid control systems on civil engineering structures, such as H_2 control (e.g. References 2–4), H_∞ control (e.g. References 5–7), sliding mode control (e.g. References 8–13), neural network,[14] etc. In particular, the theory of sliding mode control (SMC) or variable structure system (VSS) was developed for robust control of uncertain nonlinear systems. Applications of continuous sliding mode control (CSMC) that does not have chattering effect[15] to the following seismic-excited structures have been studied: (i) linear and non-linear or hysteretic buildings,[8–12] (ii) sliding isolated buildings,[16] and (iii) parametric control, such as the use of active variable dampers (AVD) on bridges,[12] and active variable stiffness (AVS) systems on buildings.[17] In addition to full state feedback controllers, static output feedback controllers using only

* Correspondence to: J. N. Yang, Department of Civil and Environmental Engineering, University of California, Irvine, CA 92717-2175, U.S.A.

Contract grant sponsor: National Science Foundation; Contract grant number: CMS-96-25616

CCC 0098–8847/97/111137–20$17·50 *Received 5 November 1996*

a limited number of sensors installed at strategic locations were also presented in the studies above. Shaking table experimental verifications of the SMC methods to linear and sliding-isolated building models have been conducted.[16,18] Based on the simulation and experimental results, it was demonstrated that the sliding mode control methods are robust and their performances are quite remarkable.

In the previous studies for SMC, the modulation of the control effort versus the response quantities was made either by adjusting the sliding surface or by specifying the maximum control level (saturated controller). This paper presents a technique for designing sliding mode controllers by introducing a fixed-order compensator using the linear quadratic optimal control theory (LQR).[19,9,20] The main advantages of using a fixed-order compensator in sliding mode control are as follows: (i) the static output feedback controller can be designed easily, (ii) the modulation of the response quantities and control efforts can be made easily in a systematic manner for both the full-state and static output feedback controllers, (iii) high-frequency components from the system response, such as acceleration feedbacks or noise, can be filtered out, and (iv) unmodelled system dynamics, such as truncated modes of the structure and higher modes in the control system, are not excited, which is important for practical implementation of control systems. The compensator is designed through the LQR formulation, which allows for the modulation of the control forces and specific response quantities in a similar manner as LQR.

Civil engineering structures, such as tall buildings and long span bridges, involve a large number of degrees of freedom. It is impractical to install sensors on every degree of freedom (or floor) to measure the full-state vector. As a result, static output feedback controllers, that utilize only the measured information from a limited number of sensors, are more desirable. However, the design of static output feedback controllers may not be easy due to the large number of degrees of freedom of the structure. On the other hand, dynamic output feedback controllers may introduce a significant time delay because it involves an on-line observer with a large dimension. An alternative approach is the use of reduced-order control. A reduced-order system (ROS) is derived from the original structural system, referred to as the full-order system (FOS), but involves a much smaller number of degrees of freedom for the purpose of the controller design. Likewise, it is much easier to design the static output feedback controller for the reduced-order system than for the full-order system.

In this paper, applications of the proposed continuous sliding mode control with a compensator (CSMC&C) are demonstrated first through numerical simulations for buildings subject to earthquakes. Then, the CSMC&C is applied to three different reduced-order systems for a tall building subject to wind turbulences and their performances are critically evaluated. Likewise, reduced-order static output feedback CSMC&C controllers are used to further reduce the number of sensors required. Simulation results indicate that the performance of the reduced-order control is very close to that of the full-order control as long as enough vibrational modes are included in the reduced-order system. Other desirable features of the reduced-order control using CSMC&C are also demonstrated.

2. FORMULATION

2.1. Equations of motion of structural systems

Consider an n degree-of-freedom linear building subject to either along-wind turbulence or one-dimensional earthquakes. The building is assumed to be symmetric and the axis of the elastic centre coincides with that of the mass centre so that there is no coupled lateral-torsional motion. The vector equation of motion is given by

$$M_s\ddot{X}(t) + C_s\dot{X}(t) + K_sX(t) = H_1U(t) + W(t) \tag{1}$$

where $X(t) = [x_1, x_2, \ldots, x_n]'$ is an n vector with $x_i(t)$ being the displacement of the designated ith floor; $U(t) = [u_1(t), u_2(t), \ldots, u_r(t)]'$ is a r-vector consisting of r control forces, and $W(t) = [w_1(t), w_2(t), \ldots, w_n(t)]'$ is an n vector denoting either the wind or earthquake-induced forces applied to the structure. In equation (1),

M_s, C_s and K_s are $(n \times n)$ mass, damping and stiffness matrices, respectively; H_1 is a $(n \times r)$ matrix denoting the location of r controllers; and a prime denotes the transpose of a vector or a matrix.

In the state space, equation (1) becomes

$$\dot{Z}(t) = AZ(t) + BU(t) + EW(t) \tag{2}$$

where $Z(t) = [z_1(t), z_2(t), \ldots, z_{2n}(t)]'$ is a $2n$ state vector; A is an $(2n \times 2n)$ linear system matrix; B is a $(2n \times r)$ controller location matrix and E is a $(2n \times n)$ excitation influence matrix given, respectively, by

$$Z(t) = \begin{bmatrix} X(t) \\ \dot{X}(t) \end{bmatrix}, \quad A = \begin{bmatrix} 0 & I \\ -M_s^{-1}K_s & -M_s^{-1}C_s \end{bmatrix}, \quad B = \begin{bmatrix} 0 \\ M_s^{-1}H_1 \end{bmatrix}, \quad E = \begin{bmatrix} 0 \\ M_s^{-1} \end{bmatrix} \tag{3}$$

The state equation for the structure in equation (2) is full-order system (FOS).

The m-dimensional output feedback vector y is expressed as

$$y = CZ(t) \tag{4}$$

where C is a $(m \times 2n)$ observation matrix.

2.2. *Continuous sliding mode control with a compensator (CSMC&C)*

The main idea of the theory of sliding mode control (SMC) is to design a controller to drive the response trajectory into the sliding surface (or switching surface) and maintain it there, whereas the motion on sliding surface is stable.[21] For systems with bounded uncertainties, SMC possesses a tremendous flexibility for compensating such uncertainties to guarantee the robustness. In the application of SMC to actuator-based control systems, it may not be easy to make a systematic trade-off between the control efforts and the structural responses. Recently, Yallapragada and Heck[19] proposed a new scheme for designing the sliding mode controller by introducing a fixed-order dynamic compensator. This approach is not only capable of modulating the control efforts and the responses, but also provides a convenient way of designing static output feedback controllers. Later, Yang *et al.*[9,20] applied this approach with slight modifications to seismic-excited structures, referred to as continuous sliding model control with compensators (CSMC&C), and obtained remarkable results. The method is presented in the following.

Design of compensator and sliding surface: A structure with the state equation in equation (2) is considered. A fixed-order compensator is introduced in the design of the sliding surface as shown in Figure. 1. The

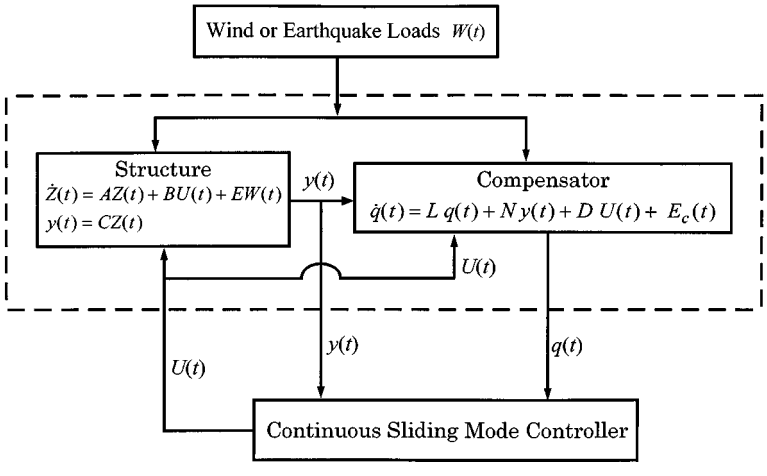

Figure 1. Block diagram of the structure–compensator-continuous sliding mode controller

minimum order of the compensator is $(r+1)$, where r is the total number of controllers. For simplicity of presentation, the order of the compensator is considered to be $(r+1)$ so that the dimension of the state vector q of the compensator is $(r+1)$, i.e. $q = [q_1, q_2']'$ where q_1 is a scalar and q_2 is a r-vector. The dynamics of the compensator is given by

$$\dot{q} = Lq + Ny + DU \tag{5}$$

where L, N and $D = [D_1', D_2']'$ are constant matrices with appropriate dimensions, D_1 is the top row vector of D, and D_2 is a $(r \times r)$ matrix. For convenience, equation (5) is chosen to be a regular form (i.e. $D_1 = 0$) and partitioned as

$$\dot{q}_1 = L_{11}q_1 + L_{12}q_2 + N_1 y \tag{6}$$

$$\dot{q}_2 = L_{21}q_1 + L_{22}q_2 + N_2 y + D_2 U \tag{7}$$

in which all submatrices have appropriate dimensions.

The state vector of the compensator is used to construct the sliding surface $S = 0$, i.e.

$$S = Pq = 0 \tag{8}$$

where $S = [s_1, s_2, \ldots, s_r]'$ is a r-vector with $s_i (i = 1, 2, \ldots, r)$ being the sliding variables. In equation (8), P is a $r \times (r+1)$ matrix partitioned as $P = [P_1, P_2]$ where P_1 is a r-column vector and P_2 is a $(r \times r)$ matrix. In the standard form of sliding mode control, P_2 is generally chosen to be an identity matrix. In the present paper, however, we would like to have the flexibility of choosing P_2. With the partition of P above, equation (8) can be written as

$$S = P_1 q_1 + P_2 q_2 = 0 \tag{9}$$

It follows from equation (9) that

$$q_2 = -P_2^{-1} P_1 q_1 \tag{10}$$

provided that P_2 is invertible. To confine the motion on the sliding surface $S = 0$, one should have $\dot{S} = 0$, i.e.

$$\dot{S} = P_1 \dot{q}_1 + P_2 \dot{q}_2 = 0 \tag{11}$$

Substituting equations (6) and (7) into equation (11) and using equation (10), one obtains the control force U, denoted by U_{eq}, as

$$U_{eq} = Gy + Hq_1 \tag{12}$$

where

$$G = -(P_2 D_2)^{-1}(P_1 N_1 + P_2 N_2) \tag{13}$$

$$H = -(P_2 D_2)^{-1}[P_1(L_{11} - L_{12}P_2^{-1}P_1) + P_2(L_{21} - L_{22}P_2^{-1}P_1)] \tag{14}$$

U_{eq} is referred to as the equivalent control force, that is the control force needed to confine (or maintain) the system on the sliding surface $S = 0$, once the system trajectory reaches $S = 0$. Substitution of the equivalent control U_{eq} into the original state equation, equation (2), the closed-loop system of the structure on the sliding surface is given by

$$\dot{Z} = AZ + BU_{eq} \tag{15}$$

where the excitation $W(t)$ has been neglected. Note that in the design of the sliding surface, the external excitation is neglected; however, it is taken into account in the design of the controller as will be described later.

Substitution of q_2 given by equation (10) into equation (6) leads to the compensator dynamics for q_1 on the sliding surface as

$$\dot{q}_1 = (L_{11} - L_{12}P_2^{-1}P_1)q_1 + N_1 y \tag{16}$$

Once q_1 is determined, q_2 can be obtained from q_1 through equation (10) and the compensator state vector q is completely defined.

Thus, the entire structure–compensator system on the sliding surface (see Figure 1), is defined by equations (15) and (16) and it has a dimension of $2n + 1$. Let us introduce the augmented state vector $\bar{Z}$ and augmented system matrices as follows:

$$\bar{Z} = \begin{bmatrix} Z \\ q_1 \end{bmatrix}, \quad \bar{y} = \begin{bmatrix} y \\ q_1 \end{bmatrix}, \quad \bar{A} = \begin{bmatrix} A & 0 \\ 0 & 0 \end{bmatrix}, \quad \bar{B} = \begin{bmatrix} B & 0 \\ 0 & 1 \end{bmatrix}, \quad \bar{U} = \begin{bmatrix} U_{\text{eq}} \\ \dot{q}_1 \end{bmatrix}, \quad \bar{C} = \begin{bmatrix} C & 0 \\ 0 & 1 \end{bmatrix} \tag{17}$$

Then, equations (15) and (16) can be cast into a $(2n + 1)$ matrix equation as follows:

$$\dot{\bar{Z}} = \bar{A}\bar{Z} + \bar{B}\bar{U} \tag{18}$$

$$\bar{y} = \bar{C}\bar{Z} \tag{19}$$

and equations (12) and (16) can be combined as

$$\bar{U} = \bar{G}\bar{y} \tag{20}$$

where

$$\bar{G} = \begin{bmatrix} G & H \\ N_1 & L_{11} - L_{12}P_2^{-1}P_1 \end{bmatrix} \tag{21}$$

P_1 and P_2 as well as the compensator characteristics will be determined from the augumented system defined by equations (18) and (19). For the augumented system in equations (18) and (19) with the static output control in equation (20), the gain matrix $\bar{G}$ can be obtained by minimizing a quadratic performance index

$$J = E\left[\int_0^\infty (\bar{Z}'Q\bar{Z} + \bar{U}'R\bar{U})\,\mathrm{d}t\right] \tag{22}$$

in which $E[\cdot]$ denotes the statistical expectation and

$$Q = \begin{bmatrix} Q_1 & 0 \\ 0 & Q_2 \end{bmatrix}, \qquad R = \begin{bmatrix} R_1 & 0 \\ 0 & R_2 \end{bmatrix} \tag{23}$$

where Q_1 and Q_2 are state weighting matrices corresponding to Z of the structure and q_1 of the compensator, respectively. Similarly, R_1 and R_2 are control weighting matrices corresponding to U_{eq} and $\dot{q}_1$, respectively. Following the optimal output feedback control theory by Levine and Athans,[22] the gain matrix $\bar{G}$ in equation (21) is obtained by solving the following non-linear matrix equations:

$$\bar{G} = -R^{-1}\bar{B}'\bar{K}\bar{L}\bar{C}'(\bar{C}\bar{L}\bar{C}')^{-1} \tag{24}$$

where

$$\bar{M}\bar{L} + \bar{L}\bar{M}' + I = 0 \tag{25}$$

$$\bar{K}\bar{M} + \bar{M}'\bar{K} + Q + \bar{C}'\bar{G}'R\bar{G}\bar{C} = 0 \tag{26}$$

$$\bar{M} = \bar{A} + \bar{B}\bar{G}\bar{C} \tag{27}$$

Equations (24)–(27) can be solved for $\bar{G}$, $\bar{L}$, $\bar{M}$, $\bar{K}$ iteratively as suggested by Srinivasa *et al.*[23] Note that when C (or $\bar{C}$) is a square matrix with a full rank, e.g. the case of full-state feedback, $\bar{G}$ and $\bar{U}$ become, respectively, $\bar{G} = -R^{-1}\bar{B}'\bar{K}\bar{C}^{-1}$ and $\bar{U} = -R^{-1}\bar{B}'\bar{K}\bar{Z}$, and $\bar{K}$ satisfies the well-known Riccati matrix equation

$$\bar{K}\bar{A} + \bar{A}'\bar{K} - \bar{K}\bar{B}R^{-1}\bar{B}'\bar{K} + Q = 0 \tag{28}$$

Once $\bar{G}$ is obtained, the following procedures can be used to compute matrices, L, N, D and P of the compensator and the sliding surface: (i) G, H, N_1 and $(L_{11} - L_{12}P_2^{-1}P_1)$ can be determined from equation (21); (ii) from equation (13) and G given, N_2 can be determined by assigning non-singular P_2, D_2 and any P_1; (iii) from equation (14) and H given, L_{21} can be determined by assigning appropriate L_{22}; (iv) Since $(L_{11} - L_{12}P_2^{-1}P_1)$ is known, L_{11} can be determined by assigning appropriate L_{12}. L_{12} and L_{22} are chosen to guarantee the stability of the open-loop augmented system as will be described later. From a conservative point of view, a stable open-loop augmented system is preferable in case the control force is saturated due to the limitation of the actuator capacity.

Design of controller: A controller is designed to drive the trajectory of the compensator into the sliding surfaces $S = 0$ and maintain it there. To achieve this goal, a Lyapunov function $V = 0.5\ S'S$ is considered. The sufficient condition for the sliding mode $S = 0$ to occur as $t \to \infty$ is $\dot{V} \leqslant 0$, i.e.

$$\dot{V} = S'\dot{S} = S'[P_1\dot{q}_1(t) + P_2\dot{q}_2(t)] \leqslant 0 \tag{29}$$

For the design of the sliding surface and compensator described previously, the external excitations have been neglected; however, they will be accounted for in the design of controller. The $(r+1)$ excitation vector to the compensator, denoted by $E_c(t)$, is considered as

$$E_c(t) = [0, E'_{12}(t)]' \tag{30}$$

in which $E_{12}(= r -$ vector) is a subset of the external excitation vector $EW(t)$ in equation (2), corresponding to the location of the controllers. In other words, elements of E_{12} are from the subset of elements of $EW(t)$, equation (2), which appears in those state equations where the control forces appear. Then, the equations for $q_2(t)$, equation (7), can be written as

$$\dot{q}_2 = L_{21}q_1 + L_{22}q_2 + N_2 y + D_2 U + E_{12} \tag{31}$$

Substituting equations (6) and (31) into equation (29), one obtains

$$\dot{V} = S'(P_2D_2)[U - U_{eq} + M_c q + D_2^{-1}E_{12}] \tag{32}$$

where U_{eq} is given by equation (12) and

$$M_c = (P_2D_2)^{-1}[(P_1L_{12}P_2^{-1}P_1 + P_2L_{22}P_2^{-1}P_1)(P_1L_{12} + P_2L_{22})] \tag{33}$$

for $\dot{V} \leqslant 0$, a possible continuous controller is given by

$$U(t) = U_{eq} - M_c q(t) - D_2^{-1}E_{12} - (P_2D_2)^{-1}\bar{\delta}S \tag{34}$$

in which $\bar{\delta}$ is a $(r \times r)$ diagonal matrix with the ith diagonal elements $\delta_i \geqslant 0$. δ_i is referred to as the sliding margin. Substitution of equation (34) into equation (32) leads to $\dot{V} = -S'\bar{\delta}S \leqslant 0$. Note that U_{eq} has been determined in equation (12).

Stability of augumented system: The state equation of the entire augmented system, including the structure, compensator and controller, in the original co-ordinate form, follows from equations (2) and (5) as

$$\dot{X}_a = A_a X_a + B_a U + E_a \tag{35}$$

where the excitation to the compensator has been included and

$$X_a = \begin{bmatrix} Z \\ q \end{bmatrix}, \quad A_a = \begin{bmatrix} A & 0 \\ NC & L \end{bmatrix}, \quad B_a = \begin{bmatrix} B \\ D \end{bmatrix}, \quad E_a = \begin{bmatrix} EW(t) \\ E_c(t) \end{bmatrix} \tag{36}$$

The controller in the preceding subsection stabilizes the closed-loop system of equation (35) for any arbitrary choices of L_{12} and L_{22}. However, the open-loop system A_a may not be stable for any choices of L_{12} and L_{22}. Methods for the determination of L_{12} and L_{22} submatrices such that the open-loop augmented system A_a is stable are available. The stability of the open-loop system is important to guarantee the stability of the structure during controller saturation. It has been found that the stability of the open-loop system and the closed-loop system with unsaturated controller are prerequisites for the stability of the closed-loop system with saturation controller. Due to the space limitation, the proof of the above statement will not be presented.

2.3. *Reduced-order system*

Civil engineering structures, e.g. high-rise buildings, long-span bridges, etc., are generally complex and consist of excessive degrees of freedom. Hence, the design of a controller, either with full-state or static output feedback, may be quite difficult. One approach is to construct a reduced-order system by retaining only the dominant eigenvalues and eigenvectors of the full-order system and the controller is designed based on the reduced-order system, referred to as the reduced-order control. Two promising reduced-order systems, i.e. the state reduced-order (SROS) and the critical-mode system (CMS), were presented and investigated by Wu[24] and Wu *et al.*[25] The state reduced-order system retains selected physical co-ordinates (state variables) and modes (eigenvalues and eigenvectors) of the FOS. Therefore, the feedback variables for the controller can be measured directly from the sensors installed on the structure. In this case, since CSMC&C controller design is based on the state reduced-order system, the control spillover and the observation spillover are not distinguishable, and hence the combined spillover effect should be examined carefully (see Reference 24). The critical-mode system retains selected modes of FOS to be controlled but uses the modal co-ordinates as the state variables. Those modal co-ordinates will be used in the design of CSMC&C controller, including the compensator design. In this case, the overall spillover effect should be taken care by appropriate compensator design to maintain stability and performance. The use of critical-mode system (CMS) in the control design for seismic-excited civil engineering structures has been presented in References 26 and 27. In addition to the reduced-order systems above, the first-mode system, i.e. retaining only one vibrational mode, will also be investigated as described in the following.

2.3.1. State reduced-order system (SROS). Consider a k-dimensional reduced-order system (ROS) with selected state variables $z_1, z_2, \ldots, z_k$, where $k < 2n$. The system matrix A of the full-order system (FOS) and matrices B and E are partitioned so that the equation (2) is expressed as

$$\begin{bmatrix} \dot{Z}_c \\ \dot{Z}_r \end{bmatrix} = \begin{bmatrix} A_c & A_{cr} \\ A_{rc} & A_r \end{bmatrix} \begin{bmatrix} Z_c \\ Z_r \end{bmatrix} + \begin{bmatrix} B_c \\ B_r \end{bmatrix} U + \begin{bmatrix} E_c \\ E_r \end{bmatrix} W \tag{37}$$

where $Z_c = [z_1, z_2, \ldots, z_k]'$ is the selected state vector of the ROS; A_c and A_r are $k \times k$ and $(2n-k) \times (2n-k)$ submatrices of A; B_c and B_r are $k \times r$ and $(2n-k) \times r$ submatrices of B; and E_c and E_r and $k \times n$ and $(2n-k) \times n$ submatrices of E. Note that one can always rearrange the state equation (2), such that the selected state variables $z_1, z_2, \ldots, z_k$ for the ROS are on the top portion of the state vector Z. The observation matrix C in equation (4) should be partitioned for the ROS as $C = [C_k, 0]$, where C_k is a $(m \times k)$-dimensional matrix and $k \geqslant m$. Thus, the state variables in the ROS preserve the same physical meanings as in the original state.

For simplicity, let the eigenvalues of A be distinct, and Λ_i and Γ_i be the ith eigenvalue and eigenvector of A, respectively. Further, let $\Gamma = [\Gamma_1, \Gamma_2, \ldots, \Gamma_{2n}]$ be the eigenvector matrix and $\Gamma^{-1} = S = [S'_1, S'_2, \ldots, S'_{2n}]'$ where S_i is the ith row vector of Γ^{-1}. The eigenvector matrix Γ is partitioned into submatrices as follows:

$$\Gamma = \begin{bmatrix} \Gamma_c & \Gamma_{cr} \\ \Gamma_{rc} & \Gamma_r \end{bmatrix} \tag{38}$$

in which, Γ_c and Γ_r are $k \times k$ and $(2n-k) \times (2n-k)$ submatrices.

Following Reference 24 and 25, the state equation of the reduced-order system, i.e. the upper part of equation (37) can be derived as

$$\dot{Z}_c = A_c^* Z_c + B_c^* U + E_c^* W \tag{39}$$

where

$$A_c^* = A_c + A_{cr}\Gamma_{rc}\Gamma_c^{-1} \tag{40}$$

$$B_c^* = \Gamma_c[S_1', S_2', \ldots, S_k']' B, \qquad E_c^* = \Gamma_c[S_1', S_2', \ldots, S_k']' E \tag{41}$$

It can be shown that the ith eigenvalue and eigenvector matrix of the reduced-order system A_c^* are equal to Λ_i $(i = 1, 2, \ldots, k)$ and Γ_c, respectively.

The output feedback of the reduced-order system (ROS) follows from equation (4) as

$$y = [C_k, 0]\begin{bmatrix} Z_c \\ Z_r \end{bmatrix} = C_k Z_c \tag{42}$$

Since the ith eigenvalue and the eigenvector matrix of A_c^* are equal to Λ_i $(i = 1, 2, \ldots, k)$ and Γ_c, the SROS retains the same eigenproperties as the first k modes of the full-order system (FOS). It can be shown easily that the SROS is completely controllable and observable if the FOS is controllable and observable for the selected k modes.[24] Note that the dimension of the SROS is the same as the number of the selected modes. Since the eigenvalues of a FOS are complex conjugates in pairs, it is necessary to choose even numbers of modes for the SROS so that A_c^*, B_c^* and E_c^* are real. Consequently, for reduced-order control, equations (39) and (42) will be used to design the CSMC&C controller rather than equations (2) and (4) described in the previous section.

2.3.2. Critical-mode system (CMS). Decoupling the state equation (2) by letting $Z = \Gamma Y$, one obtains

$$\dot{Y} = \Lambda Y + \bar{B}U + \bar{E}W \tag{43}$$

in which the eigenvalue matrix $\Lambda = \Gamma^{-1} A \Gamma$ is diagonal for distinct eigenvalues; $\bar{B} = \Gamma^{-1} B$; $\bar{\mathrm{E}} = \Gamma^{-1} E$, and Y is the modal co-ordinate vector. Equation (43) can be partitioned into

$$\begin{bmatrix} \dot{Y}_c \\ \dot{Y}_r \end{bmatrix} = \begin{bmatrix} \Lambda_c & 0 \\ 0 & \Lambda_r \end{bmatrix}\begin{bmatrix} Y_c \\ Y_r \end{bmatrix} + \begin{bmatrix} \bar{B}_c \\ \bar{B}_r \end{bmatrix} U + \begin{bmatrix} \bar{E}_c \\ \bar{E}_r \end{bmatrix} W \tag{44}$$

where Y_c and Y_r are k and $(2n - k)$ vectors, respectively; and the diagonal eigenvalue matrices, Λ_c and Λ_r, contain the first k and the remaining $(2n - k)$ eigenvalues, respectively. The k modes involved in the upper part of equation (44) with subscript c are referred to as the 'critical modes', and the lower part of equation (44) with subscript r as the 'residual modes'. The upper part of equation (44), called the critical-mode system (CMS), will be used to design the controller, referred to as critical-mode control. It can be shown easily that if the FOS is controllable and observable for the selected k modes, the CMS is completely controllable and observable. The critical-mode system in equation (44) is complex, since eigenvalue and eigenvector matrices are all complex. For controller design, these equations can be converted into the real form easily as long as the number of the critical modes, k, is chosen to be even (see Reference 25).

The measurable output vector y, equation (4), can be expressed as $y = CZ = C\Gamma Y = C_c Y_c + C_r Y_r$, where $C_c = C[\Gamma_1, \Gamma_2, \ldots, \Gamma_k]$ and $C_r = C[\Gamma_{k+1}, \Gamma_{k+2}, \ldots, \Gamma_{2n}]$. Hence, y is approximated by the construction from the critical modes only, i.e.

$$y \doteq C_c Y_c \tag{45}$$

For reduced-order control, instead of equations (2) and (4), equation (45) and the upper part of equation (44), i.e. the critical-mode equation, should be used to design the CSMC&C controller. Since the residual modes are not taken into account in the design of the controller, they may be excited by the controller, as observed

from the term $\bar{B}_r U$ in equation (44), resulting in the so-called control spillover. In addition, the observation spillover will be introduced through the measured output y contributed from the residual modes, i.e. $C_r Y_r$. Hence, the compensator should be appropriately designed to minimize the spillover effects.

2.3.3. First-mode system (FMS). Consider a building with proportional damping and equipped with an active mass damper on the jth floor. The equation of motion for the mass damper can be expressed as

$$m_d \ddot{x}_d + c_d \dot{x}_d + k_d x_d = -m_d \ddot{x}_j - u \tag{46}$$

in which x_d is the mass damper displacement w.r.t. the jth floor; m_d, c_d and k_d are the mass, damping and stiffness of the mass damper, respectively, and u is the control force generated by the actuator.

The main idea for the first-mode reduction method is to decompose the second-order equations of motion for the structures without the active mass damper into the modal co-ordinate system.[28,29] Then, the first-mode system consists of the equation of the first vibrational mode and the equation of the mass damper in equation (46), i.e. a two-degree-of-freedom system. Let ω_i, Φ_i and M_i^* be the ith eigenvalue, eigenvector and generalized mass, respectively, of the structure without the mass damper, where the equation of motion is given by equation (1). Because of the proportional damping, equation (1) is decoupled into the modal co-ordinate, i.e. into n second-order uncoupled equations. Further, we adjust the first eigenvector Φ_1 such that its jth component is equal to 1·0, and approximate the response vector X by the first mode only, i.e. $X \doteq \Phi_1 \eta_1$, where η_1 is the first modal co-ordinate. Then, it can be shown easily that the displacement x_j of the jth floor, on which the mass damper is installed, is equal to η_1, i.e. $x_j = \eta_1$. Combining the resulting first modal equation with the mass damper equation in equation (46) and replacing η_1 by x_j, one obtains

$$\begin{bmatrix} \ddot{x}_j \\ \ddot{x}_d \end{bmatrix} + \begin{bmatrix} 2\xi_1\omega_1 & -2\mu\xi_d\omega_d \\ -2\xi_1\omega_1 & 2(1+\mu)\xi_d\omega_d \end{bmatrix} \begin{bmatrix} \dot{x}_j \\ \dot{x}_d \end{bmatrix} \begin{bmatrix} \omega_1^2 & -\mu\omega_d^2 \\ -\omega_1^2 & (1+\mu)\omega_d^2 \end{bmatrix} \begin{bmatrix} x_j \\ x_d \end{bmatrix} = \begin{bmatrix} (M_1^*)^{-1} \\ -(m_d)^{-1} - (M_1^*)^{-1} \end{bmatrix} u + \begin{bmatrix} F_1 \\ -F_1 \end{bmatrix} \tag{47}$$

where $\omega_d = (k_d/m_d)^{1/2}$ and $\xi_d = c_d/2m_d\omega_d$ are the frequency and damping ratio of the mass damper; $\mu = m_d/M_1^*$ is the mass ratio with respect to the first modal mass M_1^* and $F_1 = \Phi_1' EW/M_1^*$ is the first generalized force. In this approach, the output feedback y consists of x_d, $\dot{x}_d$, x_j and $\dot{x}_j$, which can be measured directly.

Although control based on the first-mode system is quite simple, it is only applicable to the case when the structural response is dominated by the first vibrational mode. As will be shown later in a numerical example, the performance of such an approach is not acceptable even for control of wind-excited structures.

3. SIMULATION RESULTS

To demonstrate the application of the method of continuous sliding mode control with compensator (CSMC&C) presented in the previous section, simulation results are presented for the response control of seismic-excited buildings and acceleration response control of tall buildings subject to strong wind turbulences.

3.1. Example 1: A three-storey scaled building

A three-storey scaled building model, in which every storey unit is identically constructed, is considered.[30] The mass, stiffness and damping coefficients of each storey unit are $m_i = 1$ metric ton, $k_i = 980$ kN/m, and $c_i = 1{\cdot}407$ kN s/m, respectively, for $i = 1, 2$ and 3. An active bracing system (ABS) is installed in the first storey unit. The El Centro earthquake (NS component) scaled to a peak ground acceleration of $0{\cdot}11g$ is used as the input excitation.

3.1.1. Design of compensator and controller. To design the compensator, the following weighing matrices are used: $Q_1 = \text{diag.}[10^5, 10^4, 10^3, 1, 1, 1]$, $Q_2 = 10{\cdot}0$, $R_1 = 0{\cdot}1498 \times 10^6$ and $R_2 = 1{\cdot}0$ in equation (23). The matrix $\bar{G}$ in equation (21), for the full state feedback case, is obtained by solving equation (28) directly. Next, we choose a stable sliding surface $S = 100q_1 + 10q_2$, i.e. $P_1 = 100$ and $P_2 = 10$. With $\bar{G}$ computed above as well as P_1 and P_2 values, we obtain matrices for the compensator and the controller following the procedures described in earlier section as

$$L = \begin{bmatrix} -3{\cdot}16, & 0{\cdot}0 \\ -968{\cdot}4, & -100 \end{bmatrix}, \qquad N = \begin{bmatrix} 0{\cdot}0, & 0{\cdot}0, & 0{\cdot}0, & 0{\cdot}0, & 0{\cdot}0, & 0{\cdot}0 \\ 201{\cdot}4, & 129{\cdot}3, & -6{\cdot}4, & 18{\cdot}4, & 12{\cdot}0, & 8{\cdot}7 \end{bmatrix}$$

and

$$D = \begin{bmatrix} 0{\cdot}0 \\ -0{\cdot}001 \end{bmatrix}$$

Noted that we have chosen $L_{12} = 0{\cdot}0$ and $L_{22} = -100$ to make the augmented open-loop system in equation (35) stable. The excitation to the compensator, $E_c(t)$, in equation (30) is $E_c(t) = [0, 0, -1]' \ddot{x}_0(t)$.

3.1.2. Performance of full state feedback controller. Within 30 s of the earthquake episode, the peak interstorey dirft, x_i, and the peak floor accelerations, $\ddot{x}_i$, are shown in columns (2) and (3) of Table I for the building structure without control. With Q_1, Q_2, R_2, D and $E_c(t)$ given above and $\delta_1 = 10$ in equation (34), the response quantities of the controlled building for various peak control forces were computed. This was accomplished by adjusting R_1. The peak response quantities, x_i, and $\ddot{x}_i$, for the controlled structure for peak control forces 3603, 2500 and 1500 N, respectively, are presented in columns (8)–(9), (12), (13) and (16), (17) of Table I, denoted by 'CSMC&C'. The peak response quantities based on the standard LQR control method for the same peak control forces are shown in columns (4), (5), (10), (11) and (14)–(15) of Table I for comparison. For the LQR method, the same Q_1 matrix shown above is used, whereas the peak control force is obtained by adjusting R_1. For the continuous sliding mode control (CSMC) without compensator,[8] only

Table I. Peak response quantities of a three-storey building model (full-state feedback)

	No control		LQR ($U = 3603$ N)		CSMC ($U = 3603$ N)		CSMC&C ($U = 3603$ N)	
	x_i	$\ddot{x}_i$	x_i	$\ddot{x}_i$	x_i	$\ddot{x}_i$	x_i	$\ddot{x}_i$
Storey No. (1)	(cm) (2)	(cm/s^2) (3)	(cm) (4)	(cm/s^2) (5)	(cm) (6)	(cm/s^2) (7)	(cm) (8)	(cm/s^2) (9)
1	1·32	308	0·11	118	0·09	135	0·10	152
2	1·01	470	0·32	183	0·31	162	0·31	175
3	0·59	577	0·24	231	0·20	199	0·22	212

	LQR ($U = 2500$ N)		CSMC&C ($U = 2500$ N)		LQR ($U = 1500$ N)		CSMC&C ($U = 1500$ N)	
	x_i	$\ddot{x}_i$	x_i	$\ddot{x}_i$	x_i	$\ddot{x}_i$	x_i	$\ddot{x}_i$
Storey No. (1)	(cm) (10)	(cm/s^2) (11)	(cm) (12)	(cm/s^2) (13)	(cm) (14)	(cm/s^2) (15)	(cm) (16)	(cm/s^2) (17)
1	0·28	121	0·22	115	0·51	160	0·47	133
2	0·32	156	0·27	139	0·42	214	0·42	202
3	0·23	222	0·18	174	0·26	257	0·25	241

the results for the peak control force of 3603 N are presented in columns (6)–(7) of Table I denoted by CSMC. As observed from Table I, the performance of the CSMC&C (with compensator) is almost the same as that of the CSMC without compensator, but it is better than that of LQR method when the peak control force is small.

3.1.3. Performance of static output feedback controller. Suppose only the responses of the first story unit, x_1 and $\dot{x}_1$, as well as $\ddot{x}_0(t)$ are measured. With the same Q_1, Q_2, R_2, D, $E_c(t)$ and δ_1 as in the case of full state feedback, numerical results for the peak response quantities are presented in columns (4)–(5) of Table II, in which the peak control forces U are obtained by varying R_1. We next use the method of LQR static output feedback[22] with the same peak control force. The results are shown in columns (2)–(3) of Table II for comparison. As observed from Table II, the performance of the LQR and CSMC&C controllers for static output feedback is about the same.

3.2. Example 2: a ten-storey steel frame building

A ten-storey moment-resisting steel frame building, idealized by a 10 DOF system and used in Reference 31, is considered. The mass of each floor is 97·92 metric tons except the mass of the top (10th) floor that is 81·63 metric tons. The first four natural frequencies are 2·41, 7·089, 11·744 and 16·761 rad/s, and the corresponding damping ratios are 0·0533, 0·0504, 0·0694 and 0·0924, respectively. The same El Centro NS (1940) earthquake with a peak acceleration scaled to $0{\cdot}3g$ is used as the input excitation. Within 30 s of the earthquake episode, the peak interstorey drifts, x_i, and peak floor accelerations, $\ddot{x}_i$, of the building are summarized in columns (2) and (3) of Table III.

To reduce the building response, a passive mass damper is installed on the top of the building. The mass of the damper is 25 per cent of the mass of the 10th floor (i.e. 2·12 per cent of the total mass of the building) and the damping ratio is 20 per cent. The damper frequency is tuned to the fundamental frequency of the building, i.e. 2·41 rad/s. With such a passive mass damper, the peak response quantities of the building and the mass damper are presented in columns (4) and (5) of Table III. The last row of Table III, denoted by 'MD', represents the peak response quantities for the mass damper. For this particular situation, the passive mass

Table II. Peak response quantities of a three-storey building model (static output feedback)

	LQR ($U = 3603$ N)		CSMC&C ($U = 3708$ N)	
Storey No. (1)	x_i (cm) (2)	$\ddot{x}_i$ (cm/s^2) (3)	x_i (cm) (4)	$\ddot{x}_i$ (cm/s^2) (5)
1	0·11	105	0·12	105
2	0·41	188	0·41	186
3	0·26	257	0·25	243
		$U = 2500$ N		
1	0·22	111	0·18	111
2	0·37	164	0·33	153
3	0·22	218	0·20	194
		$U = 1500$ N		
1	0·39	132	0·47	139
2	0·40	190	0·42	203
3	0·24	238	0·24	232

Table III. Peak response quantities of a 10-storey building equipped with an active mass damper

	No control		TMD		CSMC&C (full-state) $U = 295$ kN		CSMC&C (Static output feedback) $U = 240$ kN		CSMC&C (Reduced-order) $U = 266$ kN	
Floor no. (1)	x_i (cm) (2)	$\ddot{x}_i$ (cm/s^2) (3)	x_i (cm) (4)	$\ddot{x}_i$ (cm/s^2) (5)	x_i (cm) (6)	$\ddot{x}_i$ (cm/s^2) (7)	x_i (cm) (8)	$\ddot{x}_i$ (cm/s^2) (9)	x_i (cm) (10)	$\ddot{x}_i$ (cm/s^2) (11)
1	3·39	271	2·81	270	2·02	271	2·01	263	1·95	261
2	3·4	275	2·82	274	2·06	279	1·98	258	1·93	249
3	3·6	281	2·99	275	2·35	282	2·22	257	2·17	244
4	3·3	278	2·72	266	2·37	271	2·26	261	2·27	262
5	3·86	288	3·47	264	2·85	224	2·65	248	2·80	263
6	4·68	287	4·1	280	3·05	194	2·80	225	3·06	223
7	5·57	257	4·88	253	3·24	211	3·06	196	3·30	173
8	5·27	260	4·68	242	2·78	213	2·81	180	2·93	174
9	5·21	334	4·67	297	2·65	240	2·84	221	2·84	278
10	3·46	408	3·16	363	2·15	230	2·19	230	1·97	256
MD	—	—	53·17	350	85·60	1397	85·01	1088	84·09	1198

damper is capable of reducing the interstorey drifts by 15 per cent, whereas the reduction for the floor acceleration is minimal.

3.2.1. Full-order system with full state feedback. To reduce the building response further, an actuator is attached to the mass damper, referred to as the active mass damper. With an active mass damper, the building response depends on the design of the controller. In designing the controller, limitations on the peak stroke and the peak control force of the actuator should be considered. A maximum stroke of 90 cm and a peak control force of 300 kN will be imposed.

The sliding mode controller with a compensator is designed for the full-order structure as follows: $Q = \text{diag.}[10, 10, 10, 10, 10, 10, 10, 10, 10, 10, 0{\cdot}025, 1, 1, 1, 1, 1, 1, 1, 1, 1, 1, 0{\cdot}001, 0{\cdot}001]$, $R = \text{diag.}[10^{-3}, 1]$, $\delta_1 = 0{\cdot}1$, $P = [1, 1]$, $L_{12} = 1{\cdot}0$, $L_{22} = -1{\cdot}0$, and $D_2 = 1{\cdot}0$. The controller is designed mainly to reduce the interstorey drifts rather than the floor accelerations. The peak interstorey drifts and peak accelerations of the building are presented in columns (6) and (7) of Table III. The peak control force of 295 kN and a peak stroke of 85·6 cm [last row of column (6)] are also shown in Table III. As observed from Table III, the active mass damper is capable of significantly reducing the interstorey drifts, in particular for the upper storey units.

3.2.2. Static output feedback. The full-state feedback controller for the full-order system, i.e. 11 DOF, presented above requires the measurements of 11 drifts and 11 velocities. To reduce the number of sensors, the static output controller is considered with the output variables $(x_3, x_6, x_{10}, x_{11}, \dot{x}_3, \dot{x}_6, \dot{x}_{10}, \dot{x}_{11})$. In other words, sensors are installed to measure the drifts and velocities of the 3rd, 6th and 10th storey units as well as the mass damper. For static output feedback, equations (25)–(27) are solved iteratively to obtain the gain matrix $\bar{G}$. The design parameters used are as follows: $Q = \text{diag.}[10, 10, 10, 10, 10, 10, 10, 10, 10, 10, 0{\cdot}001, 1, 1, 1, 1, 1, 1, 1, 1, 1, 1, 0{\cdot}001, 0{\cdot}001]$, $R = \text{diag.}[10^{-3}, 1]$ and $\delta_1 = 1{\cdot}0$. The sliding surface P and the matrices D_2, L_{12} and L_{22} are identical to that of the full-state feedback in the previous case. Within 30 seconds of the earthquake episode, the peak response quantities are presented in the columns (8) and (9) of Table III. A comparison between the results in columns (6) and (7) and the results in columns (8) and (9) of Table III indicates that the performance of the static output controller is slightly better than that of the full-state controller.

3.2.3. Reduced-order controller. For the original building with an AMD, the system matrix A is (22×22). To simplify the design procedures, a state reduced-order system described previously will be constructed and the reduced-order controller will be designed. Based on the Fourier spectrum of the El Centro earthquake, the first three vibrational modes of the building and the damper mode should be included in the state reduced-order system. The state variables chosen for the state reduced-order system are $(x_3, x_6, x_{10}, x_{11}, \dot{x}_3, \dot{x}_6, \dot{x}_{10}, \dot{x}_{11})$ and the first four pairs of complex eigenvalues are retained in the SROS. Following the system reduction scheme, equation (39), we obtain a reduced-order system with a state vector $Z = [x_3, x_6, x_{10}, x_{11}, \dot{x}_3, \dot{x}_6, \dot{x}_{10}, \dot{x}_{11}]'$. A full-state controller for such a state reduced-order system is designed. In other words, drifts and velocities of the 3rd, 6th and 10th storey units and of the mass damper are measured.

The sliding surface P and the matrices D_2, L_{12} and L_{22} are identical to that of the previous case. Q and R matrices are chosen as follows: $Q = \text{diag.}[10, 10, 10, 0{\cdot}001, 1, 1, 1, 0{\cdot}001, 0{\cdot}001]$ and $R = \text{diag.}[10^{-4}, 1]$. With $\delta_1 = 0{\cdot}1$, the peak interstorey drifts and peak floor accelerations are presented in columns (10) and (11) of Table III. As observed from Table III, the performance of the reduced-order controller is slightly better than that of the full-state controller based on the full-order system, columns (6) and (7) of Table III.

3.3. Example 3: control of wind-excited 40-storey building

Different active control techniques of tall buildings subject to strong wind turbulences have been studied in the literature (e.g. References 32–34, 4, 29, 24, 25). Active control of a 40-storey building subject to wind turbulences will be considered to illustrate the application of sliding mode control with compensator based on different reduced-order systems. Under wind turbulences, tall buildings do not have safety problems. The purpose of control systems is to reduce the discomfort of the occupants and damages to sensitive equipments or non-structural components in the building. As a result, the main objective of control is to reduce the acceleration response, rather than the interstorey drifts of the building.

The wind velocity can be decomposed into an average wind velocity and a wind fluctuation, that has been modelled as a stationary random process. Although the wind load depends on the response of the structure, the interaction effect can usually be neglected, and the wind load can be computed from the wind velocity. Hence, the wind load consists of a static load due to the average wind velocity and a dynamic load due to wind fluctuation. Consequently, the structural response is a superposition of a static response due to the static load and a dynamic response (with zero mean) due to the dynamic wind load. Since the computation of the static response is very simple and the floor acceleration is due to the dynamic load, only the dynamic response will be considered. The well-known Davenport wind load spectrum will be used herein. The cross-power spectral density of the dynamic wind loads w_i on the ith floor and w_j on the jth floor in the along wind motion can be expressed as [35]

$$S_{w_i w_j}(\omega) = \frac{8\bar{w}_i \bar{w}_j k_0 V_r^2}{\bar{V}_i \bar{V}_j |\omega|} \frac{(600\omega/\pi V_r)^2}{[1 + (600\omega/\pi V_r)^2]^{4/3}} \exp\left(-\frac{c_1 |\omega|}{2\pi} \frac{|z_i - z_j|}{V_r} \right) \tag{48}$$

where the frequency ω is in radian per second; z_j is the height of the jth floor;

$$\bar{w}_j = 0{\cdot}5\, \rho A_j C_D \bar{V}_j^2 \tag{49}$$

is the average wind force (static force) on the jth floor; V_r is the reference mean wind velocity (m/s) at 10 m above the ground; c_1 and k_0 are constants; ρ is the air density; A_j is the tributary area of the jth storey unit; and C_D is the drag coefficient that depends on structural shapes. The mean wind velocity $\bar{V}_j$ on the jth floor is assumed to follow a power law

$$\bar{V}_j = V_g (z_j / z_g)^{\alpha} \tag{50}$$

where z_g is the gradient height; V_g is the average wind velocity at the gradient height; and α is a constant between 0·15 and 0·5. The values for the parameters z_g and α can be found in Reference 35, which are

characterized by the ground condition, such as the roughness. The wind load spectrum given by equations (48)–(50) has been used for active control of wind-excited tall buildings.[33,34,24,25,37]

Given the cross-power spectral density in equation (48), sample functions of wind loads acting on every floor can be simulated. Then, sample functions of the acceleration response of each floor can be computed for buildings with and without control, referred to as the deterministic analysis. On the other hand, equation (48) can be used directly in random vibration analyses to determine the root-mean square (rms) of the acceleration response, referred to as the stochastic analysis.

Each storey unit of the 40-storey building is identically constructed with a storey height of 4 m, mass $m_i = 1290$ t, stiffness $k_i = 10^6$ kN/m, and damping $c_i = 14260$ kN s/m for $i = 1, 2, \ldots, 40$. The damping ratios and natural frequencies for the first five vibrational modes are 0·77, 2·31, 3·84, 5·37, 6·9 per cent and 1·08, 3·238, 5·391, 7·536, 9·670 rad/s, respectively. The building is symmetric in both lateral directions and the mass centre coincides with the elastic centre, so that there is no coupled lateral-torsional motions. Only the along-wind motion will be considered. The parameters used in the Davenport wind spectrum, equation (48), are as follows: $k_0 = 0{\cdot}03$, $c_1 = 7{\cdot}7$, $\alpha = 0{\cdot}4$, air density $\rho = 1{\cdot}23$ kg/m^3, drag coefficient $C_D = 1{\cdot}2$, gradient height $z_g = 300$ m, and $V_r = 11{\cdot}46$ m/s (or $V_g = 44{\cdot}694$ m/s). The tributary area for each storey of the building, A_j, is 192 m^2. Both deterministic and stochastic analyses have been conducted. In the deterministic analysis, sample functions of wind loads acting on every floor are simulated from the cross-power spectral density.[24,25] The duration of the sample functions is 300 s, which is enough to capture the statistical behaviour of wind excitations. Time histories of the building response have been computed through numerical integrations in the time domain.

To reduce the discomfort of occupants or to prevent damages to sensitive equipments, a tuned mass damper is installed on the top of the building. The mass of the damper used is 258 t, which is 20 per cent of the floor mass or 0·5 per cent of the building mass. A viscous damper with a 15 per cent damping ratio and a spring tuned to the first natural frequency of the structure are used. The corresponding stiffness and damping coefficient of the mass damper are 300·9 kN/m and 83·592 kN s/m, respectively. The displacement vector X in the equation of motion, equation (1), is expressed in terms of the absolute displacement of each floor ($i = 1, 2, \ldots, 40$); however, the relative displacement (stroke, $i = 41$) with respect to the top floor is used for the mass damper.

The peak acceleration responses of the 40-storey building without the tuned mass damper are presented in columns (2), (3) of Table IV, denoted by 'No control'. For simplicity, only the responses of the 1st, 10th, 20th, 30th, 40th floors are presented for illustration. In Table IV, $\ddot{x}$ is the peak acceleration of the floor subject to a set of simulated sample functions of wind forces and $\sigma_{\ddot{x}}$ denotes the root-mean square (rms) of acceleration of the floor based on the stochastic analysis. With the tuned mass damper, the percentages of reduction for the peak and rms accelerations with respect to the uncontrolled responses are shown in columns (4) and (5) of Table IV, denoted by 'passive damper'. The peak stroke, x_d, and the rms stroke, σ_{x_d}, are also shown above columns (4) and (5). In what follows, the peak value, $\ddot{x}$, and the rms, $\sigma_{\ddot{x}}$, of the acceleration response will be expressed by the percentages of the response reduction with respect to the uncontrolled response in columns (2) and (3) of Table IV. The results for the passive mass damper show that for higher floors the reduction for the peak acceleration is about 20–25 per cent, whereas the reduction for $\sigma_{\ddot{x}}$ is about 35–40 per cent. The discrepancy in the control performance between the stochastic and deterministic analyses has been expected because of sampling fluctuations.

For an active mass damper, an actuator is connected between the tuned mass damper and the top floor. The performances of continuous sliding mode control with compensator, denoted by CSM&C, combined with different reduced-order systems, will be evaluated and compared with each other in the following. With an active mass damper, the building response depends on the design of the controller. Two practical limitations for the actuator capacity has been considered: (i) the peak control force is about 200 kN, and (ii) the peak stroke is about 75 cm. The stroke is the relative displacement between the mass damper and the 40th floor. In terms of the rms values, the rms of the control force is about 66 kN and that of the stroke is about 25 cm.

Table IV. Peak acceleration responses and acceleration reductions of a 40-storey building

	No control		Passive damper $x_d = 21{\cdot}60$ cm $\sigma x_d = 7{\cdot}21$ cm		CSMC&C (full-order) $x_d = 72{\cdot}46$ cm $\sigma x_d = 20{\cdot}30$ cm $U = 161$ kN $\sigma_U = 51{\cdot}8$ kN		CSMC&C (first-mode) $x_d = 73{\cdot}01$ cm $\sigma x_d = 19{\cdot}58$ cm $U = 167$ kN $\sigma_U = 47{\cdot}1$ kN	
Floor no. (1)	$\ddot{x}$ (cm/s^2) (2)	$\sigma_{\ddot{x}}$ (cm/s^2) (3)	$\ddot{x}$ (%) (4)	$\sigma_{\ddot{x}}$ (%) (5)	$\ddot{x}$ (%) (6)	$\sigma_{\ddot{x}}$ (%) (7)	$\ddot{x}$ (%) (8)	$\sigma_{\ddot{x}}$ (%) (9)
1	1·09	0·36	8·3	8·3	7·3	25·0	7·3	5·6
10	6·80	2·07	21·8	26·1	48·7	53·6	30·1	27·1
20	9·00	3·35	23·3	36·1	39·0	58·8	35·6	49·0
30	11·16	4·26	24·0	40·0	45·5	60·3	37·9	54·4
40	13·51	4·78	25·0	36·0	54·8	60·9	36·1	47·5

3.3.1. Full-order state feedback control. With the actuator limitations above, a state feedback controller based on the full-order system (FOS) for CSMC&C is designed using the following control parameters: Q and R are diagonal matrices with $Q_{ii} = 1$, $i = 1, \ldots, 40$, $Q_{41,41} = 17$, $Q_{jj} = 100$, $j = 42, \ldots, 81$, $Q_{82,82} = 0{\cdot}01$, $Q_{83,83} = 1$, $R_{11} = 9 \times 10^{-14}$ and $R_{22} = 1$; $P = [1, 1]$; $L_{12} = 1$ and $L_{22} = -1$; $\delta_1 = 100$; $D_2 = 1$. Columns (6) and (7) of Table IV present the percentages of acceleration reduction based on the CSMC&C control algorithm. As observed from Table IV, the acceleration reduction increases by 20–30 per cent over the passive tuned mass damper case. The peak control force, U, the peak stroke, x_d, the rms control force, σ_U, and the rms stroke, σ_{x_d}, are also shown above columns (6) and (7). The acceleration power spectral densities of the 40th floor are presented in Figure 2, in which the light dotted curve denotes the response using the passive tuned mass damper. The solid curve in Figure 2 represents the response based on the full-order state feedback controller. Figure 2 clearly shows that the full-order state feedback controller can effectively reduce every vibrational mode of the structural response, in particular the response reduction for the second mode is quite significant. Since the full-state feedback controller is designed based on the FOS, the results in columns (6) and (7) of Table IV will be used as the basis for evaluating the merit of different reduced-order controllers.

3.3.2. State reduced-order control (SROC). The full-state feedback controller for the full-order system presented above requires the measurements (or estimates by an observer) of 82 state variables, which is not practical for implementations. The reduced-order control, which requires fewer measurements, is considered herein. Three different state reduced-order system (SROS), i.e. 10-mode, 6-mode and 4-mode systems, will be considered in conjunction with the CSMC&C control algorithm to examine their performances. The 10-mode SROS includes the lowest 10 modes (i.e. 10 eigenvalues and 10 eigenvectors) of the full-order system (FOS). Since eigenvalues and eigenvectors are complex conjugate in pairs, the 10-mode SROS consists of the first 4 vibrational modes from the building and one vibrational mode from the mass damper. The state variables for 10-mode SROS consist of the original states corresponding to the displacements and velocities of the 10th, 20th, 30th, 40th floors and the mass damper, i.e. $Z_c = [x_{10}, x_{20}, x_{30}, x_{40}, x_{41}, \dot{x}_{10}, \dot{x}_{20}, \dot{x}_{30}, \dot{x}_{40}, \dot{x}_{41}]'$. The 6-mode SROS consists of the first 2 vibrational modes from the building and one vibrational mode from the mass damper. The state variables are the displacements and velocities of the 20th, 40th floors and the mass damper. For the 4-mode SROS, the first vibrational mode of the building and the mass damper mode are chosen. The state variables consist of the displacements and velocities of the 40th floor and the

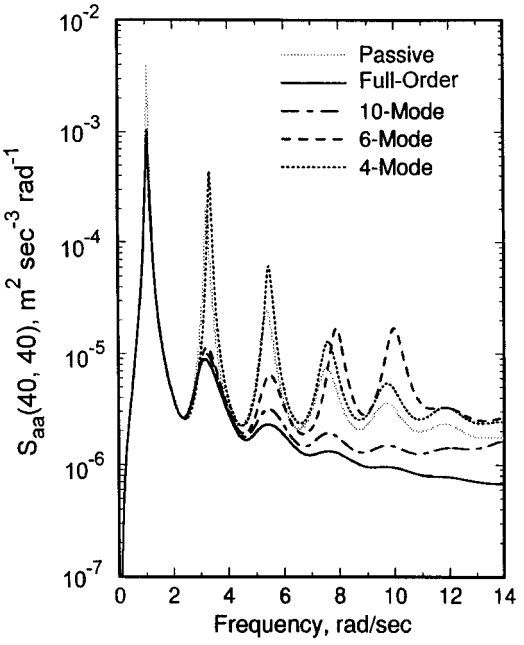

Figure 2. Acceleration power spectral density of 40th floor using CSMC&C controllers

mass damper. Since the state variables for SROS are not excessive, the full-state feedback controller will be designed. Therefore, for a 10-mode system, 10 sensors are used to measure 10 state variables. Similar situations apply to 6-mode and 4-mode systems.

The control parameters for the 10-mode, 6-mode and 4-mode SROSs are as follows: (i) 10-mode system: $Q = \text{diag}[1, 1, 1, 1, 2{\cdot}2, 100, 100, 100, 100, 0{\cdot}01, 1]$, $R = \text{diag}[10^{-13}, 1]$, $P = [1, 1]$, $D_2 = 1$, $L_{12} = 1$, $L_{22} = -1$ and $\delta_1 = 100$; (ii) 6-mode system: $Q = \text{diag}[1, 1, 1{\cdot}4, 100, 100, 0{\cdot}01, 1]$, $R = \text{diag}[10^{-13}, 1]$, $P = [1, 1]$, $D_2 = 1$, $L_{12} = 1$, $L_{22} = -1$ and $\delta_1 = 100$; (iii) 4-mode system: $Q = \text{diag}[1, 1{\cdot}1, 100, 0{\cdot}01, 1]$, $R = \text{diag}[10^{-12}, 1]$, $P = [1, 1]$, $D_2 = 1$, $L_{12} = 1$, $L_{22} = -1$ and $\delta_1 = 100$. Percentages of acceleration reductions for the building, including deterministic and stochastic analysis results, are presented in the columns (2)–(7) of Tables V for CSMC&C controllers. The acceleration power spectral densities of the 40th floor based on SROS are displayed in Figure 2. The results for 10-mode, 6-mode and 4-mode SROC are denoted by the dashed-dot curve, dashed curve, and dotted curve, respectively. Note that the first peak in Figure 2 consists of the first building mode and the mass damper mode. However, since these two vibrational modes are very close to each other, they are not distinguishable graphically.

The importance of the contribution of higher modes to the building acceleration has been demonstrated by Kareem.[36] For this 40-storey building equipped with a passive mass damper, the contribution of the higher modes (e.g. 2nd vibrational mode) is more important for the lower floor (e.g. 1st–10th floors) than for the higher floors (e.g. 20–40th floors).[24] It is conceivable that reduced-order controllers may cause spillovers in higher modes. For wind-excited buildings with active control, a good controller should be able to suppress the first few modes, or at least to avoid serious spillovers in higher modes. The results presented in Table V and Figure 2 indicate that the 10-mode and 6-mode SROCs are able to suppress the building response under wind excitations, because higher modes have been included in the SROSs. However, the degradation of the control performance becomes significant as the system is further reduced to the 4-mode SROS. As observed from Figure 2 and Table V, the performance for 10-mode SROC is quite close to that of the full-order full-state feedback control. Although the 6-mode controller is slightly less effective in controlling

Table V. Acceleration reductions using state reduced-order CSMC&C controllers

	10-mode control $x_d = 71{\cdot}38$ cm $\sigma x_d = 19{\cdot}83$ kN $U = 152$ kN $\sigma_U = 49{\cdot}5$ kN		6-mode control $x_d = 69{\cdot}32$ cm $\sigma x_d = 18{\cdot}97$ cm $U = 164$ kN $\sigma_U = 48{\cdot}3$ kN		4-mode control $x_d = 71{\cdot}44$ cm $\sigma x_d = 19{\cdot}13$ cm $U = 165$ kN $\sigma_U = 46{\cdot}1$ kN		10-mode control with 2 sensors $x_d = 71{\cdot}40$ cm $\sigma x_d = 21{\cdot}18$ cm $U = 101$ kN $\sigma_U = 28{\cdot}8$ kN	
Floor no. (1)	$\ddot{x}$(%) (2)	$\sigma_{\ddot{x}}$(%) (3)	$\ddot{x}$(%) (4)	$\sigma_{\ddot{x}}$(%) (5)	$\ddot{x}$(%) (6)	$\sigma_{\ddot{x}}$(%) (7)	$\ddot{x}$(%) (8)	$\sigma_{\ddot{x}}$(%) (9)
1	8·3	25·0	8·3	11·1	7·3	5·6	7·3	13·9
10	50·1	53·1	50·9	51·2	29·1	25·6	45·6	38·6
20	39·0	57·9	39·0	55·8	34·8	48·7	39·0	54·6
30	44·7	59·2	40·1	56·8	37·5	54·2	49·7	59·2
40	52·1	57·7	50·3	52·7	35·6	47·1	50·8	54·0

the higher modes, the performance is quite reasonable. It is further observed from Figure 2 that for the 4-mode SROC, the second, third and fourth peaks are excited due to the spillover effect and the performance is not satisfactory, especially for the lower floors (see Table V). Therefore, a reduced-order system consisting of only the first vibrational mode and the damper mode (i.e. 4-mode SROS) is not enough, although the acceleration response of the 40th floor is dominated by the first peak in Figure 2.

It should be mentioned that the response reduction for the first vibrational mode of the structure (first peak in Figure 2) has been limited by the actuator capacity, i.e. the peak stroke and peak control force. If the capacities of both the stroke and control force (or even the mass ratio) are increased, the first peak will be reduced much more significantly. In this case, the reduction for the higher modes by the controllers becomes even more important. Consequently, in constructing the reduced-order system for wind-excited tall buildings, enough higher modes should be included to avoid the spillover effects.

3.3.3. First-mode control. The first-mode system, equation (47), consists of the mass damper dynamics and the first vibrational mode of the building with proportional damping. In this case, four measurements are required, i.e. the displacements and velocities of the top floor and the mass damper. In fact, the 4-mode state reduced-order control and this first-mode control are similar approaches, although the derivations are slightly different. Based on such a first-mode control, equation (47), the control parameters are as follows: $Q = \mathrm{diag}[1, 1{\cdot}1, 100, 0{\cdot}01, 1]$, $R = \mathrm{diag}[10^{-12}, 1]$, $P = [1, 1]$, $D_2 = 1$, $L_{12} = 1$, $L_{22} = -1$ and $\delta_1 = 100$. These parameters are chosen to maintain the peak stroke around 75 cm and the peak control force around 200 kN. Deterministic and stochastic response quantities of the controlled structure have been computed. Percentages of acceleration reduction are presented in columns (8) and (9) of Table IV. As observed, the performance is about the same as that of the 4-mode state reduced-order control presented in Table V. Consequently, such a control approach is not satisfactory due to the spillover effect.

3.3.4. Critical-mode control (CMC). Simulation results based on critical-mode control are presented for the purpose of comparing the control performance with that of the state reduced-order control. For critical-mode control, the weighting matrix Q is assigned to the full-order system and the resulting weighting matrix for the modal co-ordinates Y_c is obtained from Q through the transformation of the eigenvector matrix Γ. In the following, Q is considered as a diagonal matrix for the full-order system. Control parameters for 10-mode, 6-mode and 4-mode critical-mode systems are as follows: (i) 10-mode system: $Q_{ii} = 1$, $i = 1, \ldots, 40$, $Q_{41,41} = 18$, $Q_{jj} = 100$, $j = 42, \ldots, 81$, $Q_{82,82} = 0{\cdot}01$, $Q_{83,83} = 1$, $R = \mathrm{diag}[10^{-12}, 1]$,

$P = [1, 1]$, $D_2 = 1$, $L_{12} = 1$, $L_{22} = -1$ and $\delta_1 = 100$; (ii) 6-mode system: $Q_{ii} = 1$, $i = 1, \ldots, 40$, $Q_{41,41} = 18$, $Q_{jj} = 100$, $j = 42, \ldots, 81$, $Q_{82,82} = 0{\cdot}01$, $Q_{83,83} = 1$, $R = \text{diag}[10^{-12}, 1]$, $P = [1, 1]$, $D_2 = 1$, $L_{12} = 1$, $L_{22} = -1$ and $\delta_1 = 100$; (iii) 4-mode system: $Q_{ii} = 1$, $i = 1, \ldots, 40$, $Q_{41,41} = 18$, $Q_{jj} = 100$, $j = 42, \ldots, 81$, $Q_{82,82} = 0{\cdot}01$, $Q_{83,83} = 1$, $R = \text{diag}[10^{-13}, 1]$, $P = [1, 1]$, $D_2 = 1$, $L_{12} = 1$, $L_{22} = -1$ and $\delta_1 = 100$. These design parameters are chosen mainly to reduce the acceleration response and to maintain a peak stroke of about 75 cm and a peak control force of about 200 kN. Again, the full-state feedback controllers are used for the critical-mode systems with the same measured feedback quantities as the SROC.

The peak response quantities based on the deterministic analysis have been computed and the percentages of peak acceleration reduction are presented in columns (2)–(4) of Table VI. As observed from Table VI, the results for the 10-mode and 6-mode controls are comparable to that of the full-order controller, whereas the acceleration reductions degrade seriously for the 4-mode control due to the spillover effect.

3.3.5. Output feedback for reduced-order systems. All controllers above are designed based on the reduced-order systems using full-state feedback. For instance, for the 6-mode ROS, 6 sensors are used to measure 6 response feedback variables. Similar situations apply to 10-mode and 4-mode ROSs. We can further reduce the number of sensors (feedback variables) for the reduced-order control by use of CSMC&C static output feedback controllers as presented in the following.

(i) *State reduced-order control (SROC)*: We consider a static output controller, based on the 10-mode SROS, in which only two sensors are used, i.e. only the measurements of the displacement and velocity of the 40th floor. The design parameters are as follows: $Q = \text{diag}\ [1, 1, 1, 1, 0{\cdot}1, 100, 100, 100, 100, 0{\cdot}01, 0{\cdot}0001]$, $R = \text{diag}[5{\cdot}0 \times 10^{-11}, 1]$, $P = [1, 1]$, $D_2 = 1$, $L_{12} = 1$, $L_{22} = -1$ $\delta_1 = 100$. Deterministic and stochastic response quantities have been computed. Percentages of acceleration reduction are presented in columns (8) and (9) of Table V, denoted by "10-mode control with 2 sensors". The results indicate that the control performance is remarkable, although only two sensors are used.

(ii) *Critical-mode control (CMC)*: Again, the 10-mode system with 2 sensors considered above is used to design the critical-mode controller. The design parameters are as follows. Q is a diagonal matrix in which $Q_{i,i} = 1$, $i = 1, 2, \ldots, 40$, $Q_{41,41} = 0$, $Q_{j,j} = 100$, $j = 42, \ldots, 81$, $Q_{82,82} = 0{\cdot}01$, $Q_{83,83} = 1{\cdot}0 \times 10^{-7}$, $R = \text{diag}[3 \times 10^{-10}, 1]$, $P = [1, 1]$, $D_2 = 1$, $L_{12} = 1$, $L_{22} = -1$ and $\delta_1 = 100$. Simulation results for the peak response quantities have been obtained. Percentages of peak acceleration reduction are presented in column (5) of Table VI. In this case, the control performance is remarkable and comparable to that of the state reduced-order control presented in column (8) of Table V.

Table VI. Acceleration reductions using critical-mode CSMC&C controllers

	10-mode control $x_d = 72{\cdot}05$cm $U = 153$ kN	6-mode control $x_d = 70{\cdot}91$ cm $U = 176$ kN	4-mode control $x_d = 70{\cdot}68$ cm $U = 243$ kN	10-mode control with 2 sensors $x_d = 74{\cdot}8$ cm $U = 109$ kN
Floor no. (1)	$\ddot{x}$(%) (2)	$\ddot{x}$(%) (3)	$\ddot{x}$(%) (4)	$\ddot{x}$(%) (5)
1	8·3	8·3	8·3	8·3
10	51·0	51·2	38·7	44·6
20	39·1	39·1	24·0	39·1
30	44·8	40·1	35·1	51·6
40	52·4	50·3	18·9	48·9

4. CONCLUSION

The design of continuous sliding mode controller with a fixed-order compensator (CSMC&C) using the theory of optimal control has been presented for applications to civil infrastructures subject to earthquakes or strong wind turbulences. The major advantages of this approach over the conventional sliding mode control are as follows: (i) it provides a simple procedure to make trade-offs between specific response quantities and control efforts, (ii) it provides systematic approach to design static output feedback controllers, that utilize only a limited number of sensors without an observer, and (iii) the compensator can be used to filter out high-frequency components of the structural response to accommodate the acceleration output feedback. The ability to systematically design CSMC&C static output feedback controller greatly facilitate the practical applications of control systems. The first two advantages of the present approach have been demonstrated through extensive simulation results. Due to space limitations, the advantage of the present approach to accommodate acceleration output (static) feedbacks will be presented elsewhere. Further, sliding mode control using dynamic output feedback has been presented recently.[37]

Civil engineering structures usually involve excessive degrees of freedom, making the controller design quite difficult. In this paper, three different reduced-order systems have been explored and the reduced-order control based on the continuous sliding mode controller with compensators (CSMC&C) have been investigated. Applications to active control of tall buildings subject to either earthquake excitations or strong wind turbulences have been demonstrated. Simulation results indicate that the performance of the controllers based on the reduced-order system is comparable to that of the controllers for the full-order system, as long as enough vibrational modes are included in the reduced-order system. The performance of the reduced-order continuous sliding mode controllers with a compensator has been shown to be quite remarkable.

ACKNOWLEDGEMENT

This research is supported by the National Science Foundation through grant numbers CMS-96-25616.

REFERENCES

1. G. W. Housner and S. F. Masri (eds), *Proc. of the First World Conf. on Structural Control*, Pasadena, CA, USC Publication, 1994.
2. S. J. Dyke and B. F. Spencer *et al.*, 'The role of control–structure interaction in predictive system design', *ASCE J. Engng. Mech.* **121**, 322–338 (1995).
3. S. J. Dyke, B. F. Spencer, P. Quest, M. K. Sain, D. C. Kaspari and T. T. Soong, 'Acceleration feedback control of MDOF structures', *ASCE J. Engng. Mech.* **122**, 907–918 (1996).
4. J. Suhardjo, B. F. Spencer and A. Kareem, 'Frequency domain optimal control of wind excited buildings', *ASCE J. Engng. Mech.* **118**, 2463–2481 (1992).
5. W. E. Schmitendorf, F. Jabbari and J. N. Yang, 'Robust control techniques for buildings under earthquake excitation', *Earthquake Engng. Struct. Dyn.* **23**(5), 539–552 (1994).
6. F. Jabbari, W. E. Schmitendorf and J. N. Yang. 'H_∞ control for seismic-excited building with acceleration feedback', *ASCE J. Engng. Mech.* **121**(9), 994–1002 (1995).
7. I. E. Kose, W. E. Schmitendorf, F. Jabbari and J. N. Yang, 'H_∞ active seismic response control using static output feedback', *J. Engng. Mech. ASCE* **122**(7), 651–659 (1996).
8. J. N. Yang, J. C. Wu and A. K. Agrawal, 'Sliding mode control for seismic-excited linear and nonlinear structures', *Technical Report NCEER-94-0017*, National Center for Earthquake Engineering Research, Buffalo, NY, 1994.
9. J. N. Yang, A. K. Agrawal and J. C. Wu, 'Sliding mode control of structures subjected to seismic loads', *Proc. 1st World Conf. on Structural Control*, Vol. 1, USC Publication, 1994, pp. WA1-13 to WA1-22.
10. J. N. Yang, J. C. Wu and A. K. Agrawal, 'Sliding mode control of nonlinear and hysteretic structures', *ASCE J. Engng. Mech.* **121**(12), 1330–1339 (1995).
11. J. N. Yang, J. C. Wu and A. K. Agrawal, 'Sliding mode control of seismically excited linear structures', *ASCE J. Engng. Mech.* **121**(12), 1386–1390 (1995).
12. J. N. Yang, J. C. Wu, K. Kawashima and S. Unjoh, 'Hybrid control of seismic-excited bridge structures', *Earthquake Engng. Struct. Dyn.* **24**(11), 1437–1451 (1995).
13. M. P. Singh, E. Matheu and L. E. Suarez, 'Active and semi-active control of structures under seismic excitation', *Earthquake Engng. Struct. Dyn.* **26**, 193–213 (1997).
14. J. Ghaboussi and A. Joyhataie, 'Active control of structures using neural networks', *J. Engng. Mech. ASCE* **121**, 555–567 (1995).
15. F. Zhou and D. G. Fisher, 'Continuous sliding mode control', *Int. J. Control* **55**, 313–327 (1992).
16. J. N. Yang, J. C. Wu, A. M. Reinhorn and M. Riley, 'Control of sliding-isolated buildings using sliding mode control', ASCE *J. Struct. Engng.* **122**(2), 83–91 (1996)

17. J. N. Yang, J. C. Wu and Z. Li, 'Control of seismic-excited buildings using active variable stiffness systems', *J. Engng. Struct.* **18**(8), 589–596 (1996).
18. J. N. Yang, J. C. Wu, A. M. Reinhorn, M. Riley, W. E. Shmitendorf and F. Jabbari, 'Experimental verifications of H_∞ and sliding mode control for seismic-excited buildings', *ASCE J. Struct. Engng.* **122(1)**, 69–75 (1996).
19. S. V. Yallapragada and B. S. Heck, 'Optimal control design for variable structure systems with fixed order compensators', *Proc. ACC*, Vol **1**, 1992, pp. 876–880.
20. J. N. Yang, J. C. Wu, A. K. Agrawal and S. Y. Hsu, 'Reduced-order sliding mode control with compenstors for seismic response control', *Proc. 11th World Conf. on Earthquake Engineering,* 23–28 June, Acapulco, Mexico, Paper No 273, 1996.
21. V. I. Utkin, *Sliding Modes in Control Optimization*, Springer, Berlin, 1992.
22. W. S. Levine and M. Athans, 'On the determination of the optimal constant output feedback gains for linear multivariable sytems', *IEEE Trans. Automatic Control*, **AC-15**, 44–48 (1970).
23. Y. G. Srinivasa and T. Rajgopalan, 'Algorithms for the computation of optimal output feedback gains', *Proc. 18th IEEE Conf. on Decision and Control,* FL, 1979, pp. 576–579.
24. J. C. Wu, 'Active control of wind-excited structures', *Ph.D. Dissertation*, University of California, Irvine, CA, 1996.
25. J. C. Wu, J. N. Yang and W. Schmitendorf, 'Reduced-order H_∞ and *LQR* control for wind-excited tall buildings', *J. Engng. Struct.*, 1997.
26. J. N. Yang and M. J. Lin, 'Optimal critical-mode control of building under seismic load', *ASCE J. Engng. Mech. Div.* **108**, (EM6), 1167–1185 (1982).
27. J. N. Juang, S. Sae-Ung and J. N. Yang, 'Active control of large building structures', in H. H. E. Leipholz (ed.), *Structural Control*, North Holland, Amsterdam, 1980, pp. 663–676.
28. J. C. H. Chang and T. T. Soong, 'Structural control using active tuned mass dampers', *ASCE J. Engng. Mech. Div.* **106** (EM 6) 1091–1098 (1980).
29. S. Ankireddi and H. T. Y. Yang, 'Simple ATMD control methodology for tall buildings subject to wind loads', *ASCE J. Struct. Engng.* **122**(1), 83–91 (1996).
30. T. Kobori, *et al.*, 'Seismic response controlled structures with active variable stiffness systems', *Earthquake Engng. Struct. Dyn.*, **22**, 925–941 (1993).
31. P. B. Shing, M. Dixon, N. Kermiche, R. Su and D. M. Frangopol, 'Hybrid control techniques for building structures', *Proc. 1st World Conf. on Structural Control,* LA, Vol. 1, 1994, pp. WP2-100 to WP2-109.
32. S. Sae-Ung and J. T. P. Yao, 'Active control of building structures', *ASCE J. Engng. Mech. Div.* **104** (EM2), 335–350 (1978).
33. J. N. Yang and B. Samali, 'Control of tall buildings in along-wind motion', *ASCE J. Struct. Engng.* **109**(1), 50–68 (1983).
34. B. Samali, J. N. Yang and C. T. Yeh, 'Control of lateral-torsional motion of wind-excited buildings', *ASCE J. Engng. Mech.* **111**(6), 777–796 (1985).
35. E. Simiu and R. H. Scanlan, *Wind Effects on Structures*, 2nd edn., Wiley, New York, 1986.
36. A. Kareem, 'Wind-excited response of buildings in higher modes', *ASCE J. Struct. Div.* **107** (ST4), 701–706 (1981).
37. J. C. Wu and J. N. Yang, 'Continuous sliding mode control of a TV transmission tower under stochastic wind', *Proceedings of the 1997 American Control Conference*, Albuquerque, NM, June 1997, Vol. 2, pp. 883–887, 1997.

